ARTICLE

Photocatalytic Degradation of Phenol over MWCNTs-TiO_2 Composite Catalysts with Different Diameters

Chen Li[a,b], Wen-dong Wang[a*]

a. Department of Chemical Physics, University of Science and Technology of China, Hefei 230026, China

b. Department of Chemistry and Chemical Engineering, Huainan Normal University, Huainan 232001, China

(Dated: Received on January 22, 2009; Accepted on April 13, 2009)

Titania-based composite catalysts were prepared through a sol-gel route employing multi-walled carbon nanotubes with different diameters. The materials were characterized using thermogravimetric analysis, nitrogen adsorption-desorption isotherm, powder X-ray diffraction, scanning electron microscopy, and diffuse reflectance UV-Vis absorption spectra. The application of the catalysts to photocatalytic degradation of phenol was tested under UV-Vis irradiation. A synergetic effect on phenol removal was observed in case of composite catalysts, which was evaluated in terms of apparent rate constant, total organic carbon removal and photonic efficiency.

Key words: Photocatalytic degradation, Phenol, Titanium dioxide, Multi-walled carbon nanotube, Composite catalyst

I. INTRODUCTION

More stringent government regulations and progressive public consciousness prompt the scientific and technological communities toward deeper research in the area of wastewater treatment and recycling. Photocatalytic degradation (PCD) processes is earning increasing importance in this area as the most effective emerging destruction technology, since these processes require mild operation conditions of temperature and pressure but result in total mineralization without any waste disposal problem [1−5]. TiO_2 has been extensively used as a photocatalyst, and a TiO_2/UV system has been widely investigated in the PCD processes, during which the activation of UV irradiation upon TiO_2 can generate electron/hole couples with strong redox properties [6]. Oxygen is often present as the electron acceptor to form the superoxide radical ion ($O_2^{\cdot -}$), while OH^- and H_2O are available as electron donors to yield the hydroxyl radical ($HO^{\cdot}$). Both of the radicals are very reactive and strongly oxidizing, capable of totally mineralizing most of the organic pollutants.

The photocatalytic efficiencies of TiO_2 particles largely depend upon their microstructure and physical properties due to different preparation conditions and methods [7−11], as well as doping with or incorporating some other elements, adsorbents or supports [12−15]. With respect to the synthesis methods, the sol-gel technique from alkoxide precursors is one of the most used, which provides a versatile synthesis route with variable operation conditions, and can be adjusted to produce titania with tailored morphological features.

It has been reported that the presence of carbon materials in TiO_2 photocatalysts can induce some beneficial effects on their photocatalytic activities [16,17]. The most recent review [18] covers the application of various carbon materials in photocatalysis during the last decade. Aside from those investigations on the TiO_2 and carbon composite photocatalysts using conventional forms of carbon such as activated carbon [19−21] and graphite [22,23], carbon nanotubes (CNTs) have gained much attention as attractive and competitive catalyst supports due to the combination of their electronic, adsorption, mechanical, and thermal properties [24]. In particular, multi-walled carbon nanotubes (MWCNTs) and TiO_2 composite catalysts have been successfully prepared by various processes [25−30], which reveals a considerable synergy effect between MWCNTs and TiO_2 on the photocatalytic degradation of organic compounds and other photoreactions in the presence of UV and visible irradiation.

On the basis of our preceding work [20,25,26], the effect of MWCNTs structure and property on the performance of MWCNTs-TiO_2 composite catalysts was further studied, and the photodegradation of phenol over MWCNTs-TiO_2 composite catalysts with different diameters of containing MWCNTs is reported in the present work.

*Author to whom correspondence should be addressed. E-mail: wangwd@ustc.edu.cn, Tel.: +86-551-3603683, FAX: +86-551-3601592

II. EXPERIMENTS

A. Catalysts preparation

Titanium isopropoxide (Aldrich, 97%) was used as alkoxide precursor to prepare the photocatalysts. Multi-walled carbon nanotubes (Shenzhen NTP, China, ≥95%) with different diameters of <10 nm, 20−40 nm, and 60−100 nm (manufacturer data) were denoted as MWCNTs1, MWCNTs2, and MWCNTs3, respectively. Degussa TiO_2-P25 was used as standard for comparison purposes whenever necessary.

MWCNTs-TiO_2 composite catalysts were prepared using an acid-catalyzed sol-gel method at room temperature as follows. 0.1 mol of $Ti(OC_3H_7)_4$ was dissolved in 200 mL of anhydrous ethanol. The solution was stirred magnetically for 30 min, and then 1.56 mL of nitric acid (65%) was added. Subsequently, certain amount of MWCNTs (20% of MWCNTs to the resulting TiO_2) was introduced into the $Ti(OC_3H_7)_4$ ethanol solution. The mixture was loosely covered and stirred continuously until a homogenous MWCNTs-containing gel formed. The gel was aged in air for several days. The resulting xerogel was crushed into fine powder and dried at room temperature. The powder was calcined at 400 °C in N_2 flow for 2 h to obtain MWCNTs-TiO_2 composite catalysts.

B. Characterization methods

The thermal behaviors of the composite materials were analyzed with a Shimadzu DTG-60 system to determine their actual carbon contents. N_2 adsorption-desorption isotherms were measured using a Coulter 3100 apparatus and the surface area was calculated by a BET method. X-ray diffraction (XRD) patterns were obtained on a Philips X'Pert Pro Super diffractometer (Cu Kα, λ=0.15406 nm). The composite catalysts were characterized by SEM using a Jeol JSM-6700F equipped with an energy dispersive X-ray (EDX) detector. The diffuse reflectance UV-Vis spectra of the solid were measured on a JASCO V-560 UV-Vis spectrophotometer with an integrating sphere attachment (JASCO ISV-469).

C. Photodegradation experiments

Catalytic activities were evaluated by photodegradation of phenol in aqueous media under UV-Vis light irradiation. The experiments were carried out in a glass immersion photochemical reactor charged with 800 mL of suspension/solution. The irradiation source (Heraeus TQ 150 medium pressure mercury vapor lamp) was located axially and held in an immersion tube. A circulating water jacket was employed to cool the lamp and cancel the infrared radiation, thus preventing any heating of the suspension. The most intense lines of the lamp with immersion tube were at 366, 436, 546, and 577 nm (manufacturer data), which features the majority of the radiation flux and light quanta in the visible region (λ>400 nm).

The initial phenol concentration (C_0') was 50 mg/L and the amount of suspended photocatalyst was kept at 1 g/L of TiO_2. In the case of the composite catalysts, the amount of solid was calculated by keeping the same concentration of TiO_2 as the carbon content changed correspondingly. The suspension was stirred at constant speed during all the photoreaction process. Before turning on the light, the suspension containing phenol and photocatalyst was magnetically stirred in a dark condition for 1 h to establish an adsorption-desorption equilibrium.

The first sample was taken out at the end of the dark adsorption period in order to determine the phenol concentration in solution, which was hereafter considered as the initial concentration (C_0) after dark adsorption. The light was then powered on and we started to count the reaction time. Samples were withdrawn regularly from the reactor and filtrated with Millipore disk (0.45 μm) to separate any suspended solid. The clean transparent solution was analyzed by the UV-Vis spectroscopy (UNICO UV-2800A). The full spectrum (200−800 nm) for each sample was recorded and the absorbance at characteristic band 270 nm was followed to determine the phenol concentration. Total organic carbon (TOC) measurements were performed on a Shimadzu TOC-VCPN analyzer to determine the degree of mineralization. Repetition of tests was done to ensure the reproducibility.

III. RESULTS AND DISCUSSION

A. Catalysts characterization

The carbon content (C_{TG}) determined by TG is listed in Table I for the series of composite materials MWCNTs-TiO_2, containing 20% weight ratio of MWCNTs to a 100 weight basis of neat TiO_2. A mass loss of about 16% is observed due to the carbon gasification, which agrees very well with the calculated value

TABLE I Characteristic of MWCNTs and TiO_2 composite materials.

Sample	C_{TG}/%	S_{BET}/(m^2/g)	d_{TiO_2}/nm
TiO_2	–	107	8.5
MWCNTs1-TiO_2	16.2	157	7.0
MWCNTs1	–	456	–
MWCNTs2-TiO_2	16.6	102	7.6
MWCNTs2	–	81	–
MWCNTs3-TiO_2	16.3	96	8.0
MWCNTs3	–	39	–

DOI:10.1088/1674-0068/22/04/423-428

from the initial ratio.

The N_2 adsorption-desorption isotherms (not shown) for TiO_2 and MWCNTs-TiO_2 composite materials can be ascribed to type IV according to IUPAC classification [31], which suggests a mesoporous pore texture [32]. With the range of MWCNTs diameter increasing from <10 nm to 20−40 nm to 60−100 nm, the BET surface area (S_{BET}) of MWCNTs decreases from 456 m^2/g to 81 m^2/g to 39 m^2/g (see Table I). In the case of MWCNTs-TiO_2 composite materials, the surface area varies due to the accordingly introduced MWCNTs. An increase in area is observed for MWCNTS1-TiO_2 compared with the neat TiO_2, while there is a slight decrease for the other two samples.

The XRD patterns (Fig.1) of different solids reveals that TiO_2 in anatase phase is the only form identified for TiO_2 and composite materials. The rutile and brookite phases of TiO_2 are not detected. It is observed that the peak widths broaden slightly for MWCNTs-TiO_2 composite materials when compared with neat TiO_2. TiO_2 crystallite size (d_{TiO_2}) estimated from the line broadening by using Scherrer's equation is also compared in Table I. The crystallite size for neat TiO_2 of 8.5 nm is obtained, while the size decreases to 7.0, 7.6, and 8.0 nm for the composite material with the increase in MWCNTs diameter.

The morphologies of MWCNTs and TiO_2 composite catalysts with different MWCNTs diameters were revealed by SEM investigation. The SEM images of MWCNTs1-TiO_2 and MWCNTs3-TiO_2 are compared in Fig.2. It is observed that relatively homogeneous MWCNTs is embedded in TiO_2 matrix. The difference of MWCNTs with different diameter is also evident. EDX analysis results confirm only the presence of C, O, and Ti elements in the composite materials.

The diffuse reflectance UV-Vis spectra of different solids are presented in Fig.3, expressed in terms of Kubelka-Munk equivalent absorption units. It is observed that the absorption spectrum of sol-gel prepared TiO_2 shifts a bit to the visible light region when compared with TiO_2-P25. Furthermore, the composite materials can absorb at higher wavelength and the absorption even covers the whole range of the measured UV-Vis region due to the introduction of MWCNTs, which may lead to the modification of the fundamental pro-

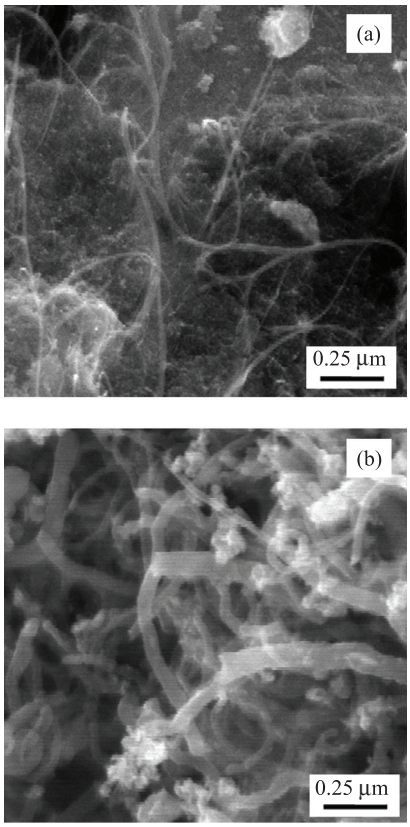

FIG. 2 SEM images of (a) MWCNTs1-TiO_2 and (b) MWCNTs3-TiO_2 composite materials.

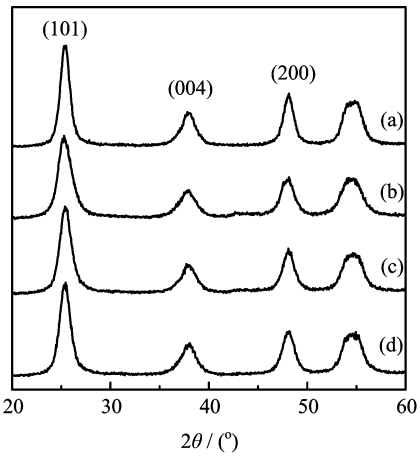

FIG. 1 The XRD of TiO_2 (a), MWCNTs1-TiO_2 (b), MWCNTs2-TiO_2 (c), and MWCNTs3-TiO_2 (d).

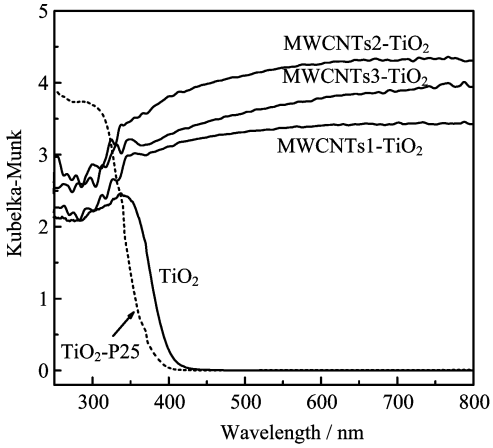

FIG. 3 Diffuse reflectance UV-Vis spectra of TiO_2-P25, TiO_2, and MWCNTs-TiO_2 composite materials.

DOI:10.1088/1674-0068/22/04/423-428

TABLE II Summary of photodegradation of phenol over different solids at given initial concentration of phenol (C_0'= 50 mg/L).

Sample	C_0/(mg/L)	$k_{app}\times10^{-3}$ min^{-1}	R	ξ_r	X_{9h}/%	X_{TOC}/%
TiO_2	47.5	1.8	–	1.0	65	66
MWCNTs1-TiO_2	43.5	6.4	3.6	3.3	96	90
MWCNTs2-TiO_2	45.6	3.4	1.9	1.6	76	74
MWCNTs3-TiO_2	46.8	2.6	1.4	1.4	69	72
TiO_2-P25	48.8	–	–	–	30	39

cess of electron/pair formation when exposed to UV-Vis irradiation.

B. Photocatalytic degradation of phenol

The photocatalytic degradation of phenol in aqueous suspension of composite catalysts containing MWCNTs and TiO_2 follows apparent first-order kinetics. The standard reaction was monitored within 3 h, and the kinetic plots are shown by linear transform in $f(t)=\ln(C_0/C)$ in Fig.4. No appreciable phenol conversion can be observed for the blank photolysis without any solid under the same reaction conditions.

It is evident that all the MWCNTs-TiO_2 composite catalysts exhibit higher phenol degradation activity than neat TiO_2. For the composite catalysts with different MWCNTs diameters, the activity increases with the decrease in MWCNTs diameter, and the MWCNTs1-TiO_2 with the smallest MWCNTs diameter shows the maximum synergetic effect. The activities of the prepared catalysts can be evaluated by comparing their apparent first-order rate constants (k_{app}) listed in Table II. A synergy factor (R) is defined to qualify the synergetic effect as [19]:

$$R = \frac{k_{app}(\text{MWCNTs-TiO}_2)}{k_{app}(\text{TiO}_2)} \tag{1}$$

The introduction of MWCNTs into TiO_2 obviously creates a kinetic synergetic effect photodegradation of phenol with an increase in k_{app} by a factor of 3.6, 1.9, and 1.4 respectively for the composite catalysts with the increase in MWCNTs diameter.

From Table II, it is also observed that all the samples show a similar phenol concentration after the 60 min dark adsorption period, which indicates an identical adsorption capacity for different solids. Different from the system of TiO_2 and activated carbon [19,20], the introduction of MWCNTs into the composite catalysts does not provide an apparent additional effect on their adsorption capacities [25,26]. Therefore, the synergetic effect induced by MWCNTs can favor not only higher rate constants but also higher reaction rates for MWCNTs-TiO_2 composite catalysts.

It is important to evaluate the photonic efficiency of the process from the point view of energy consumption

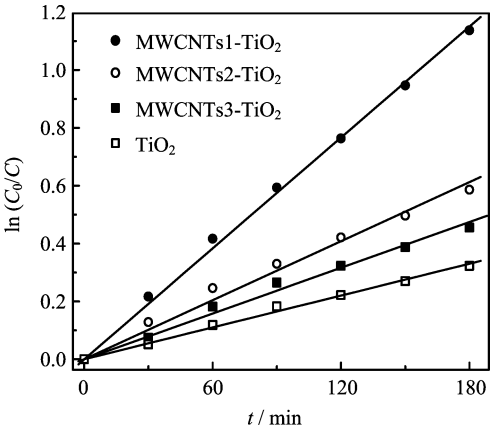

FIG. 4 Apparent first-order linear transform $f(t)=\ln(C_0/C)$ kinetic plots for photocatalytic degradation of phenol over TiO_2 and MWCNTs-TiO_2 composite catalysts.

by the definition of quantum yield [33]. From the kinetics standpoint, the initial quantum yield (ϕ_0) can be defined as the ratio of the reaction rate (r_0) to the efficient photo flux (ϕ) [34]. The value of quantum yield may vary in a wide range, according to the characteristics of catalysts, the experimental conditions and especially the nature of the reactions under consideration. In order to compare the photonic efficiency of the process over different photocatalysts, the relative photonic efficiency (ξ_r) [35] can be suggested as

$$\xi_r = \frac{\phi_0(\text{MWCNTs-TiO}_2)}{\phi_0(\text{TiO}_2)} \tag{2}$$

Considering the present photocatalytic processes under identical experimental conditions, this value may be calculated as:

$$\xi_r = \frac{r_0(\text{MWCNTs-TiO}_2)}{r_0(\text{TiO}_2)} \tag{3}$$

where r_0 can be obtained from the corresponding values of C_0 and k_{app} in Table II. Consistent with the evolution of the synergy factor, the result displays the advantage of the introduction of MWCNTs into TiO_2, which features higher photonic efficiency during the photocatalytic process, especially a pronounced relative photonic efficiency of 3.3 in the presence of MWCNTS1-TiO_2.

DOI:10.1088/1674-0068/22/04/423-428

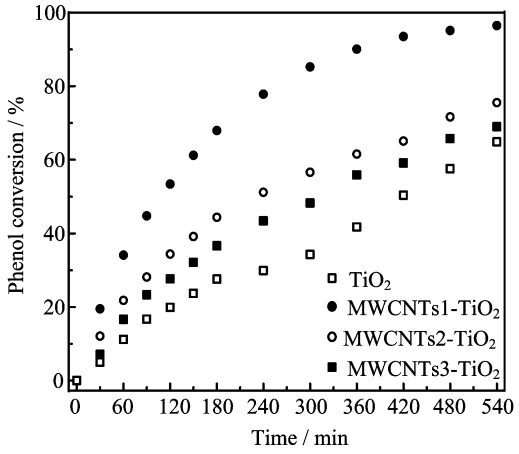

FIG. 5 Phenol removal during long-term photodegradation reactions over TiO_2 and MWCNTs-TiO_2 composite catalysts.

During a long-term running photodegradation reaction (Fig.5), the complete disappearance of phenol (more than 95% conversion) over MWCNTS1-TiO_2 can be achieved within 9 h. By contrast, phenol conversion after 9 h of photoreaction (X_{9h}) over different solids is also seen in Table II as well as the TOC removal results X_{TOC}. The commercially available TiO_2-P25 shows phenol conversion of 30%, while all the sol-gel prepared catalysts reveal much better performances with more than double conversion after 9 h of irradiation, which is also in line with the TOC removal results.

With the exception of acting as an adsorbent or dispersing agent, it is more reasonable to ascribe the observed synergetic effect of MWCNTs-TiO_2 composite catalysts to MWCNTs acting as a photosensitizer [36]. Taking into account the semiconducting property of carbon nanotubes, MWCNTs may absorb the irradiation and inject the photo-induced electron into the TiO_2 conduction band. This charge transfer was experimentally supported by other observations of enhanced photocurrent for the composite materials containing carbon and TiO_2 [36−39]. The electron transfer can trigger the formation of superoxide radical ion $O_2^{\cdot -}$ and hydroxyl radical $HO^{\cdot}$, which are very reactive radicals and responsible for the degradation of the organic compound.

IV. CONCLUSION

MWCNTS-TiO_2 composite photocatalysts containing MWCNTs with different diameters were prepared using a modified sol-gel process. Material characterization indicates a relatively homogeneous MWCNTs dispersion in nanocrystallite TiO_2 matrix with modified UV-Vis absorption properties, suggesting a strong interphase structure effect between MWCNTs and TiO_2 in the composite materials. Synergetic effect on the photocatalytic degradation of phenol was observed over MWCNTs-TiO_2 composite catalysts, which exhibit higher photocatalytic activity and photonic efficiency in comparison with neat TiO_2 and commercially available P25. The decrease in MWCNTs diameter enhances the synergetic effect on photocatalytic degradation of phenol. The observed synergetic effect may be explained in terms of the intimate contact between MWCNTs and TiO_2 phases, and MWCNTs might act as a photosensitizer in the composite catalysts.

V. ACKNOWLEDGMENT

This work was supported by the National Natural Science Foundation of China (No.20703042).

[1] J. C. Zhao, C. C. Chen, and W. H. Ma, Top. Catal. **35**, 269 (2005).
[2] P. R. Gogate and A. B. Pandit, Adv. Environ. Res. **8**, 501 (2004).
[3] I. K. Konstantinou and T. A. Albanis, Appl. Catal. B **49**, 1 (2004).
[4] D. Chatterjee and S. Dasgupta, J. Photochem. Photobiol. C **6**, 186 (2005).
[5] J. M. Herrmann, Top. Catal. **34**, 49 (2005).
[6] O. Legrini, E. Oliveros, and A. M. Braun, Chem. Rev. **93**, 671 (1993).
[7] S. Sakthivel, M. C. Hidalgo, D. W. Bahnemann, S. U. Geissen, V. Murugesan, and A. Vogelpohl, Appl. Catal. B **63**, 31 (2006).
[8] K. Y. Jung, S. B. Park, and H. D. Jang, Catal. Commun. **5**, 491 (2004).
[9] X. X. Fan, T. Yu, L. Z. Zhang, X. Y. Chen, and Z. G. Zou, Chin. J. Chem. Phys. **20**, 733 (2007).
[10] M. C. Yan, F. Chen, J. L. Zhang, and M. Anpo, J. Phys. Chem. B **109**, 8673 (2005).
[11] H. Kominami, S. Murakami, J. Kato, Y. Kera, and B. Ohtani, J. Phys. Chem. B **106**, 10501 (2002).
[12] Q. Li, R. Xie, E. A. Mintz, and J. K. Shangw, J. Am. Ceram. Soc. **90**, 3863 (2007).
[13] L. Wan, J. F. Li, J. Y. Feng, W. Sun, and Z. Q. Mao, Chin. J. Chem. Phys. **21**, 487 (2008).
[14] X. Y. Li, D. S. Wang, G. X. Cheng, Q. Z. Luo, J. An, and Y. H. Wang, Appl. Catal. B **81**, 267 (2008).
[15] S. N. Hosseini, S. M. Borghei, M. Vossoughi, and N. Taghavinia, Appl. Catal. B **74**, 53 (2007).
[16] S. U. M. Khan, M. Al-Shahry, and W. B. Ingler, Science **297**, 2243 (2002).
[17] S. Sakthivel and H. Kisch, Angew. Chem. Int. Ed. **42**, 4908 (2003).
[18] J. L. Faria and W. D. Wang, *Carbon materials in photocatalysis*, in P. Serp and J. L. Figueiredo, Eds., Carbon Materials for Catalysis, John Wiley & Sons, 579 (2008).
[19] J. Matos, J. Laine, and J. M. Herrmann, Appl. Catal. B **18**, 281 (1998).
[20] W. D. Wang, C. G. Silva, and J. L. Faria, Appl. Catal. B **70**, 470 (2007).
[21] G. L. Puma, A. Bono, D. Krishnaiah, and J. G. Collin, J. Hazard. Mater. **157**, 209 (2008).

DOI:10.1088/1674-0068/22/04/423-428

[22] L. W. Zhan, H. B. Fu, and Y. F. Zhu, Adv. Funct. Mater. **18**, 2180 (2008).
[23] Z. B. Lei, Y. Xiao, L. Q. Dang, W. S. You, G. S. Hu, and J. Zhang, Chem. Mater. **19**, 477 (2007).
[24] P. Serp, M. Corrias, and P. Kalck, Appl. Catal. A **253**, 337 (2003).
[25] W. D. Wang, P. Serp, P. Kalck, and J. L. Faria, Appl. Catal. B **56**, 305 (2005).
[26] W. D. Wang, P. Serp, P. Kalck, C. G. Silva, and J. L. Faria, Mater. Res. Bull. **43**, 958 (2008).
[27] Y. Yao, G. Li, S. Ciston, R. M. Lueptow, and K. A. Gray, Environ. Sci. Technol. **42**, 4952 (2008).
[28] B. Liu and H. C. Zeng, Chem. Mater. **20**, 2711 (2008).
[29] C. Y. Yen, Y. F. Lin, C. H. Hung, Y. H. Tseng, C. C. Ma, M. C. Chang, and H. Shao, Nanotechnology **19**, 11 (2008).
[30] G. M. An, W. H. Ma, Z. Y. Sun, Z. M. Liu, B. X. Han, S. D. Miao, Z. J. Miao, and K. L. Ding, Carbon **45**, 1795 (2007).
[31] K. S. W. Sing, D. H. Everett, R. A. W. Haul, L. Moscou, R. A. Pierotti, J. Rouquerol, and T. Siemieniewska, Pure Appl. Chem. **57**, 603 (1985).
[32] G. Leofanti, M. Padovan, G. Tozzola, and B. Venturelli, Catal. Today **41**, 207 (1998).
[33] A. M. Braun, M. T. Maurette, and E. Oliveros, *Photochemical Technology*, 2nd Edn., Chichester: John Wiley & Sons, 580 (1991).
[34] J. M. Herrmann, Catal. Today **53**, 115 (1999).
[35] N. Serpone, J. Photochem. Photobiol. A **104**, 1 (1997).
[36] C. Lettmann, K. Hildenbrand, H. Kisch, W. Macyk, and W. F. Maier, Appl. Catal. B **32**, 215 (2001).
[37] P. V. Kamat, I. Bedja, and S. Hotchandani, J. Phys. Chem. **98**, 9137 (1994).
[38] S. Banerjee and S. S. Wong, Nano Lett. **2**, 195 (2002).
[39] K. H. Jung, J. S. Hong, R. Vittal, and K. J. Kim, Chem. Lett. 864 (2002).

DOI:10.1088/1674-0068/22/04/423-428